

# Slurry sample injection for determination of ferrite nanocolloids chemical composition by ICP spectrometry

M. H. Sousa<sup>\*</sup>, E. S. Lins<sup>\*</sup>, F. A. Tourinho<sup>\*</sup>, J. Depeyrot<sup>\*\*</sup>  
G. R. de Castro<sup>\*\*\*</sup>, W. D. Martins<sup>\*\*\*\*</sup>, C. F. S. Castro<sup>\*\*\*\*</sup> and L. F. Zara<sup>\*\*\*\*</sup>

<sup>\*</sup>Grupo de Fluidos Complexos, Instituto de Química, Universidade de Brasília  
CP 04478, CEP 70904-970, Brasília-DF, Brazil, fralda@unb.br

<sup>\*\*</sup>Grupo de Fluidos Complexos, Instituto de Física, Universidade de Brasília  
CP 04455, CEP 70904-970, Brasília-DF, Brazil

<sup>\*\*\*</sup>Departamento de Física e Química, Universidade Estadual Paulista  
CP 31, CEP 15385-000, Ilha Solteira-SP, Brazil.

<sup>\*\*\*\*</sup>Laboratório de Espectroscopia Aplicada, Universidade Católica de Brasília  
Campus I, QS 07 Lote 01, CEP 71966-700, Brasília-DF, Brazil

## ABSTRACT

This work proposes a new method to determine the chemical composition of magnetic ferrite nanoparticles by the slurry injection technique using the inductively coupled plasma optical emission spectroscopy. In this way, experimental conditions such as aerosol gas flow rate and colloidal stability were optimized in order to use aqueous calibration curves in the slurry nebulization and to determine the chemical composition of a series of sols containing chemically synthesized size-tailored NiFe<sub>2</sub>O<sub>4</sub> nanograins. Then, the results of direct sampling and those of conventional aqueous introduction analysis are compared, showing the efficiency of the proposed method.

**Keywords:** ferrite nanoparticle, magnetic colloid, slurry injection, icp-oes

## 1 INTRODUCTION

The miniaturization of components in order to construct new devices is an essential feature of modern technology. Consequently, the bottom-up routes towards nanometer-scale are becoming largely utilized to achieve new functional materials with applications from electronics to the medicine. In particular, the spinel ferrite nanoparticles are important magnetic materials that are widely appreciated in industry and in biomedical field<sup>1</sup>. Moreover, the surface of these oxides is extremely reactive to attach functional molecules or to generate a superficial density of charge which permits the dispersion of the nanograins into several non-polar or polar matrixes. In that case, when conveniently dispersed in a liquid to form the magnetic fluids (or ferrofluids), these nanograins have their properties enhanced since in solution they possess more degrees of freedom than in powder or film forms<sup>2</sup>.

In addition, when their surfaces are conveniently modified through the adsorption of biomolecules, such

nanograins have promising applications in drug delivery, cell separation and advanced clinical uses in cancer diagnosis and treatment<sup>3</sup>. Since most of these applications require dynamical characterization of nanograins in blood and tissues probes, instrumental chemical methods like atomic absorption and plasma emission spectroscopy have been utilized as practical tools to analyze the composition of these samples<sup>4,5</sup>. However, these procedures require an acidic dissolution of the nanoparticles before the chemical analysis, a step which induces loss or sample contamination.

By the way, the slurry introduction technique has been of increasing interest for analysis of a wide range of materials from inorganic to biological samples<sup>6</sup>. Actually, there are advantages and concerns when slurries are used. The advantages are that the preparation is simple (so contamination can be minimized), no aggressive reagents are needed, it is relatively quick and calibration can be done using aqueous standards. About the concerns, it is important to keep in mind that if accurate analyses are to be obtained using the slurry technique, the particles should be as small as possible, the slurry must present a high colloidal stability and the maximum amount of solid sample in the slurry must be kept low to ensure its stability and low viscosity.

In this work, we demonstrate a simpler and less aggressive method which minimizes sample digestion and undesired effects using the inductively coupled plasma optical emission spectroscopy (ICP-OES). In this way, size-tailored NiFe<sub>2</sub>O<sub>4</sub> nanograins were first chemically synthesized using “bottom-up” method and after they were peptized electrostatically into aqueous solution to form stable sols. Furthermore, the crystallographic structure and crystalline size of the nanograins were determined by x-ray diffractometry.

The principle of analysis route was three fold: First, the chemical composition of NiFe<sub>2</sub>O<sub>4</sub> nanograins samples was analyzed by direct injection of the nanomaterials (as

slurries) in the ICP device. Second, the experimental conditions such as aerosol gas flow rate and colloidal stability were optimized in order to use aqueous conventional calibration curves in the proposed slurry nebulization technique. Third, the results of direct sampling and aqueous introduction analysis were statistically compared, showing the reliability of the proposed method.

## 2 EXPERIMENTAL

### 2.1 Samples

The magnetic fluid samples were synthesized by following the procedure described in literature<sup>7</sup>. Ferrite nanoparticles were prepared by alkalizing 1:2 mixtures of 1 mol/L Ni<sup>2+</sup> and Fe<sup>3+</sup> at 100°C, under vigorous stirring. Changes in velocity of mixing of reactants allow to obtain nanoparticles with different mean sizes. Then, particles were electrostatically peptized in aqueous media, using particle surface treatment. Thus, in order to refine the size-sorting, the synthesized samples were centrifuged at 4000 RPM during 15 minutes. After centrifugation, the resulting precipitate and supernatant were redispersed, forming stable sols of high quality.

### 2.2 Structure characterization

The crystalline structure of solids and their crystalline sizes were determined by x-ray diffraction experiments (XRD) realized on powder samples after evaporation of the sol. Measurements were performed by x-ray diffractometer in a conventional Rigaku-Geigerflex generator operating at 40 kV/30 mA and Cu-K $\alpha$  radiation selected by a graphite monochromator. X-ray powder diffraction data were obtained in a 2 $\theta$  scanning range from 25° to 80° with a step size of 0.05° (2 $\theta$ ) with 8 s counting time at each step. The average crystal size ( $d_{XR}$ ) was deduced by means of the Scherrer formula from the width at half maximum of the diffraction line (311).

### 2.3 Chemical analysis

ICP-OES measurements were carried out using a Varian-Liberty Sequential ICP atomic emission spectrometer, equipped with a Sturman-Masters nebulizer chamber coupled with a V-groove nebulizer and radial torch, operated under the following guidelines: power – 1.2 KW; plasma flow – 15 L/min; auxiliary flow – 1.5 L/min; nebulizer pressure – 200 KPa; viewing height – 10 mm; pump rate – 15 rpm. Iron and nickel were analyzed at 259.837 and 221.647 nm respectively. The determination of metal content in the nanoparticles was compared using two distinct procedures of sample injection into the ICP torch. In the first method (the standard method), concentrated HCl was utilized to completely dissolve the nanoparticles and then distilled water was introduced to vary the

concentration into the range of the calibration curve. In the second method, the colloidal sols were diluted at constant pH (in order to assure a maximum colloidal stability) and directly introduced into the torch. In this work, the first method is referred as aqueous introduction (AI) and the second as slurry introduction (SI). Moreover, each sample was analyzed in quadruplicate. A Levene test was conducted for homogeneity of variance in the samples and Student's t test for unpaired observations was used for the statistical evaluation of differences. A probability (P) value below 0.05 was considered to be statistically significant.

## 3 RESULTS AND DISCUSSION

Four nickel ferrite nanoparticle based samples were chosen to perform the study that was proposed in this work. The crystallographic structure of the nanograins was investigated by x-ray diffractometry showing that only spinel phase was identified for all the samples (see Figure 1). The mean nanograin crystalline sizes are listed in Table 1 and were obtained through the Scherrer formula.

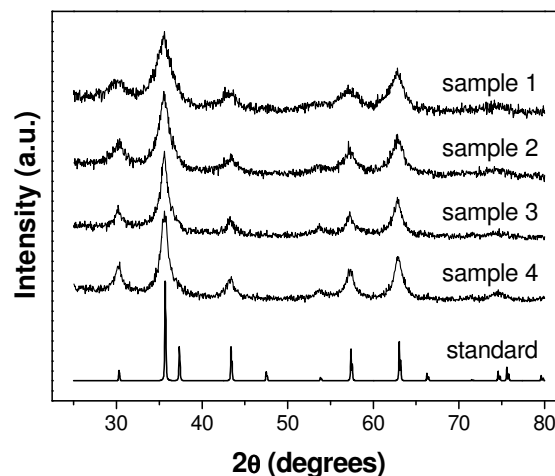


Figure 1: XRD patterns of synthesized nanoparticle samples compared with a bulk standard material.

In order to characterize chemically the samples, 100  $\mu$ L of each ferrofluid were treated with 1 mL of concentrated HCl to complete dissolution of nanoparticles. Then, after dilution to the calibration curve range (0-250 and 0-500 mg/L for Ni<sup>2+</sup> and Fe<sup>3+</sup> respectively) samples were analyzed using ICP-OES and the instrumental conditions described in the experimental section. The metal concentrations using aqueous introduction and determined from ICP-OES are summarized in Table 1, which also brings the sample concentrations obtained from atomic absorption spectroscopy (AAS) measurements. Statistical analysis showed that ICP results are reliable when compared to those obtained from the standard AAS method.

Sample		1	2	3	4
$d_{XR}$ (nm)		4.2	6.0	7.5	9.0
ICP-OES	$Fe^{3+}$	323.22	288.25	244.45	238.22
	(mg/L)	(1.35)	(1.24)	(1.21)	(1.18)
OES	$Ni^{2+}$	64.71	62.05	56.40	58.73
	(mg/L)	(0.56)	(0.61)	(0.62)	(0.50)
AAS	$Fe^{3+}$	321.60	286.66	246.86	237.84
	(mg/L)	(1.63)	(1.15)	(1.35)	(1.27)
AAS	$Ni^{2+}$	64.38	61.71	56.95	58.64
	(mg/L)	(0.68)	(0.52)	(0.74)	(0.88)
$R_M$		5.25	4.88	4.56	4.26

Table 1: Mean and standard deviation for metal concentrations determined from ICP-OES and AAS, using aqueous introduction.  $R_M$  is molar ratio between  $Fe^{3+}$  and  $Ni^{2+}$  in the nanoparticle and  $d_{XR}$  is the mean crystalline nanoparticle diameter obtained from XRD experiments.

Furthermore, for all samples investigated here the molar ratio between  $Fe^{3+}$  and  $Ni^{2+}$  was greater than 2, the expected value taking into account the stoichiometry of the ferrite  $NiFe_2O_4$ . This divergence is assumed to be due to the treatment with  $Fe(NO_3)_3$  during the synthesis step which creates a layer rich in iron on particle surface<sup>8</sup>.

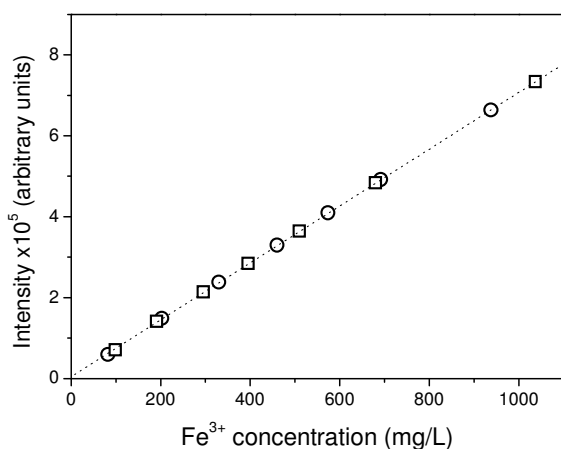


Figure 2: Emission intensity as a function of the true  $Fe^{3+}$  concentration for samples 1 (○) and 4 (□) using the slurry injection technique by ICP-OES.

By the way, the slurry introduction technique was checked by direct injection of synthesized colloid (suitably diluted to the calibration range) into the ICP torch. In this case, the intensity showed a linear dependence on the true metal nanoparticle concentrations for all samples into the calibration curve range. This is shown in Figure 2, a plot of the emission intensity versus the  $Fe^{3+}$  concentration (for samples 1 and 4) in which all the points fit a line passing through the origin. This strongly indicates that the signal obtained from this SI method is quantitatively equivalent to

the one acquired from aqueous introduction, using the same experimental conditions.

Moreover, signal intensity of SI technique was optimized through the pH adjustment. In this way, samples were diluted to the desired pH, left for 30 minutes and then analyzed by ICP-OES. Figure 3 shows that the relative intensity is maximal at pH's around 2 and 12, but minimal at pH = 8. The difference between maximum and minimum intensity is about 10 % (in absolute values) as the sample pH varies from 1 to 13. These results can be associated to the pH-dependent colloidal stability of the slurry<sup>9</sup>. In fact, ferrite nanoparticles are efficiently peptized only into acidic or basic media. In neutral medium, close to the point of zero charge, the system flocculates. These phenomenological considerations reveal the pH-dependence of the surface charge density of the particles which at low (high) pH values are positively (negatively) charged. For extreme pH values where the particle surface becomes saturated (pH < 4 and pH > 10) the intensity reaches the maxima since the slurry is more stable. Close to the neutral pH, where the surface charge is very small to ensure a sufficient repulsion, particles settle and as a consequence the intensity decreases.

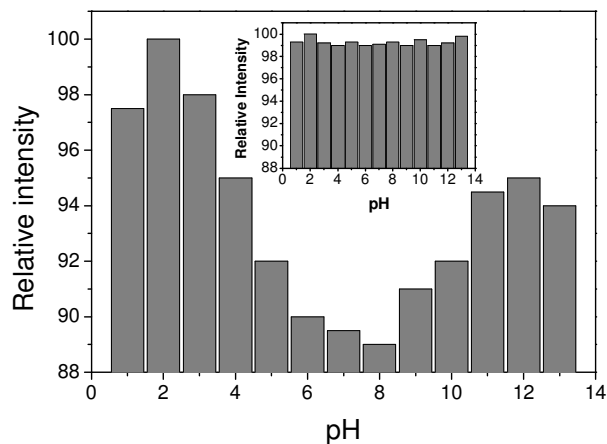


Figure 3: Relative intensity for  $Fe^{3+}$  emission as a function of the pH (sample 4). The inset shows these relative intensities for freshly homogenized slurries.

However, when this analysis is made using freshly homogenized samples, the intensity variation decreases to less than 2 % (see the inset on Figure 3) indicating that, probably due to the reduced size of the nanograins, the slurry easily becomes homogeneous by thermal agitation.

The results of the chemical dosages using aqueous and slurry introduction were then compared. In this way, Table 2 lists the mean metal concentration as well as the standard deviation for each sample, using both injection methods. Levene's test indicated that all samples analyzed by SI and AI procedures presented equal variances. In addition, Student's t test for unpaired observations was conducted,

demonstrating equivalence between the results obtained with either SI or AI analytic procedures (no  $P < 0.05$  was observed).

Sample	$C_{Fe}$ (mg/L)	$S_{Fe}$ (mg/L)	$C_{Ni}$ (mg/L)	$S_{Ni}$ (mg/L)	
1	229.39	1.32	45.92	0.18	SI
	230.18	1.10	46.08	0.22	AI
2	201.78	1.03	43.44	0.09	SI
	201.74	0.79	43.43	0.13	AI
3	219.65	0.94	50.67	0.19	SI
	218.00	1.02	50.29	0.14	AI
4	125.38	0.22	30.91	0.07	SI
	125.09	0.56	30.84	0.13	AI

Table 2: Results of ICP-OES for AI and SI techniques.  $C_{Fe}$  and  $C_{Ni}$  are respectively the mean  $Fe^{3+}$  and  $Ni^{2+}$  concentrations and  $S_{Fe}$  and  $S_{Ni}$  their standard deviations.

Finally, Figure 3 shows the correlation between the  $Fe^{3+}$  and  $Ni^{2+}$  normalized concentrations, determined for the samples randomly diluted into the calibration range by AI and SI methods. For both metals, all the experimental points bear to a line with slope 1 and that pass through the origin. This strongly indicates that, in this range of nanoparticle size and using these experimental conditions, the diameter of the nanograins had no influence in the slurry analysis.

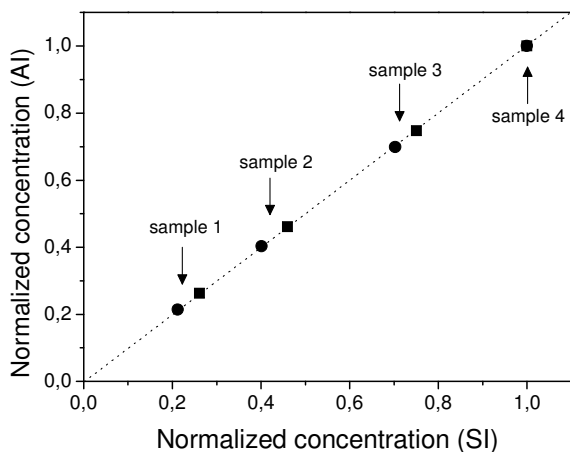


Figure 1: Correlation between normalized concentrations of  $Fe^{3+}$  (■) and  $Ni^{2+}$  (●) using the SI and AI by ICP-OES.

## 4 CONCLUSIONS

In this work, sol samples based on  $NiFe_2O_4$  nanoparticles were chemically synthesized and characterized. A size-sorting procedure rendered samples with nanoparticles ranging from 4.2 to 9 nm. The experimental apparatus conditions and the slurry stability were optimized in view of quantitatively determining nanoparticle composition, using slurry sample injection by ICP-OES. Best results were obtained with sol samples diluted at constant pH to assure maximum colloidal stability. Statistical tests indicate that the differences between the metal concentrations determined using aqueous and slurry sample introduction were not significant. Finally, in the case of the samples studied here, slurry sample introduction offered many advantages over the conventional AI technique such as reduced sample pretreatment time, lesser possibility of contamination and use of simple direct calibration with aqueous solutions.

## 5 ACKNOWLEDGEMENTS

The authors thank the Brazilian agency CNPq for financial support, proposal numbers 473224/2004-6 and 555161/2005-6.

## REFERENCES

- [1] A. J. Freeman, S. D. Bader (Eds.), "Magnetism Beyond 2000", North-Holland, 1999.
- [2] V. E. Fertman, "Magnetic Fluids Guidebook: Properties and Applications", Hemisphere Publishing Corporation, 1990.
- [3] C. C. Berry, A. S. G. Curtis, J. Phys. D: Appl. Phys., 36, R198, 2003.
- [4] R. Itri, J. Depeyrot, F. A. Tourinho, M. H. Sousa, Eur. Phys. J. E, 4, 201, 2001.
- [5] M. H. Sousa, F. A. Tourinho; J. Depeyrot, G. J. Silva, M. C. F. L. Lara, J. Phys. Chem., 105, 1168, 2001.
- [6] J. A. C. Broekaert, "Analytical Atomic Spectrometry with Flames and Plasmas", 120, Wiley-VHC, 2002.
- [7] M. H. Sousa, F. A. Tourinho, J. Depeyrot, E. Dubois, R. Perzynski, Progr. Colloid Polym. Sci., 128, 109, 2004.
- [8] J. C. O. Silva, M. H. Sousa, F. A. Tourinho, J. C. Rubim, Langmuir, 18, 5511, 2002.
- [9] A. F. C. Campos, F. A. Tourinho, G. J. da Silva, M. C. F. L. Lara, J. Depeyrot, Eur. Phys. J. E, 6, 29, 2001.